

INFLUENCE OF THE ENERGY PARAMETERS OF THE PRIMARY CIRCUIT ON THE CURRENT CHARACTERISTICS OF THE DIN-2K ACCELERATOR

D.V. Vinnikov^{1,2}, V.V. Katrechko¹, O.M. Ozerov¹, V.I. Tkachev¹, S.V. Marchenko¹,
V.B. Yuferov¹, O.V. Manuilenko^{1,3}

¹National Science Center “Kharkov Institute of Physics and Technology”, Kharkiv, Ukraine;

²O.Ya. Usikov Institute for Radiophysics and Electronics of the NAS of Ukraine,
Kharkiv, Ukraine;

³V.N. Karazin Kharkiv National University, Kharkiv, Ukraine

E-mail: vinniden@gmail.com

Optimal voltage values were established for plasma guns and the pulsed current generator providing maximum break current values. The current values were determined for the plasma jumper formation region. The optimal time delay between the triggering of the plasma guns and the pulsed current generator has been established. The beam current was measured in the region behind the vacuum diode and in the plasma jumper region. The ultimate current was determined for the available plant geometry.

PACS: 52.75.-d, 94.20. wc, 52.80 Vp, 52.70Kz, 29.30Ep

INTRODUCTION

Accelerating equipment operating based on the principle of plasma opening switch (POS) or plasma current breakers (PCB) is widely used in various industrial, high-tech and scientific fields [1, 2]. The DIN-2K plant is a high-current linear electron accelerator [3, 4]. Similar systems used as pulsed microwave generators operating on the basis of an inductive energy storage device with a plasma current breaker ensure the small size of the entire system, in contrast to bulky Arkadiev-Marx generator-based accelerators, with power exceeding 500 MW in the frequency range of 1 to 25 GHz and the efficiency factor of up to 10% or linear accelerators based on impulse voltage generators [5 - 7]. The advantages of such systems are the ability to work without a focusing magnetic field and the ability to quickly change the output characteristics of radiation pulses (pulse repetition rate, pulse generation rate, and the signal strength).

The main factors of influence on the materials, the environment and the objects located both in the immediate vicinity of the region of initiation of physical processes and at a considerable distance include the beam of charged particles and the virtual cathode (VC) being formed. Electron accelerators with VC are implemented to create powerful microwave devices and are used by radiation and biological technologies for the pulsed radiation sterilization, destruction of rocks, modification of the surfaces of solid materials, and as a source of ions for implantation and hardening [8]. Microwave radiation is the most important output influencing factor, and the power and energy of it depend on the break current value, on the vacuum diode geometry (VD), the initial energy parameters of the primary circuit, namely the energy of plasma guns (PG), pulsed current generator (PCG), time delays and vacuum conditions.

Therefore, the study of the effect of energy parameters on the characteristics of the break current is of substantive scientific interest.

The objectives of this research are to establish the optimal ranges for energy parameters of the primary circuits of the power supply systems used by the high-current linear accelerator DIN-2K that guarantee the maximum values of the break current and its implementation at a maximum rise in the plasma jumper current.

1. STATEMENT OF THE PROBLEM

The current dynamics was studied in different sections of the DIN-2K high-current electron accelerator (Fig. 1).

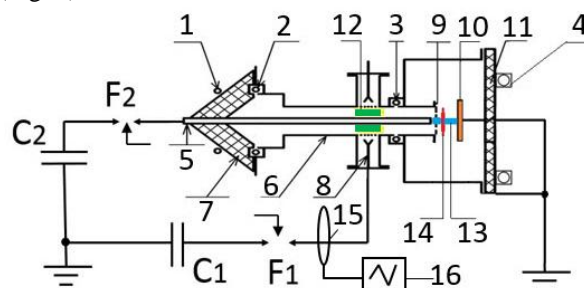


Fig. 1. General view of the DIN-2K accelerator:
1 – Rogovsky belt № 1; 2 – Rogovsky belt № 2;
3 – Rogovsky belt № 3; 4 – Rogovsky belt № 4;
5 – tubular cathode of 26 mm in diameter;
6 – the chamber body as the anode of the coaxial line of the accelerator; 7 – high-voltage insulator;
8 – a block of plasma guns – 5 pieces; 9 – grid-anode;
10 – copper current collector; 11 – end plexiglass flange; 12 – plasma jumper; 13 – electron beam;
14 – VC at the beam current exceeding the limit;
15 – Rogovsky belt № 5; 16 – oscilloscope; C1, F1 – tank and the air-controlled gun discharger; C2, F2 – tank and the air-controlled PCG unit discharger

To initiate the discharge in the plant, a block of plasma guns C1, up to 16 kV and PCG C2 up to 40 kV was triggered. After the controlled actuation of the PG-8, a breakdown occurs through the discharger F1 along the surface of the guns. The plasma (12) formed as a result of the breakdown is injected into the chamber (6)

filling it mainly due to the gas-kinetic expansion and the pressure gradient. The chamber body is the anode with a stepped-like changing diameter. In front of the mesh, the diameter is 98 mm and it expands after it to 290 mm. The diameter expansion reduces the probability of the microwave breakdown along the surface of the plexiglass flange 11 onto the chamber body. Plasma jets of the guns propagate at the initial moment of time into a cone with an angle of up to 60° and a speed of $(2...7) \cdot 10^6$ cm/s, depending on the charging voltage value. After about 3 μs, the plasma reaches the accelerator cathode (5) of 26 mm diameter and being partially reflected from it and filling the chamber relatively evenly. The plasma density can be considered conventionally uniform over the entire cross section. Subsequently, the plasma spreads in both directions along the cathode-anode axis. On elapse of the time set on the block, i.e. 3 to 30 μs, the energy accumulated in the IK50/3 capacitors of the PCG begins to release in the cathode-anode gap after the discharger F2 is triggered. To prevent the breakdown in the area near the discharger F2, a high-voltage insulator of 50 kV is placed between the anode and cathode. The magnetic energy accumulation time is defined by the current rise front and does not exceed 1 μs. The current flowing through the jumper creates, in its turn, a magnetic field that pushes electrons out of the plasma. Faster electrons rush to the anode and at some time point the conductivity is broken in such a way that an abrupt increase in resistance occurs, current instability is formed and the so-called “break” of the current occurs, resulting in the voltage multiplication [1, 9, 10]. This voltage jump provides an explosive emission of electrons from the cathode actuating the particle acceleration phase. An electron beam is formed, accelerated by the grid-anode field, with a geometric transparency of 0.6. Electrons passing through the grid are accelerated and then slowed down by their own field, creating thus a potential well in the form of a space charge, creating a VC (14). The VC formation is possible only at beam currents above the so-called limiting vacuum current:

$$I_{scl}(kA) = \frac{8.5}{\ln \frac{r_0}{r_b}} \left(\left(1 + \frac{V_0(MV)}{0.511} \right)^{\frac{2}{3}} - 1 \right)^{3/2},$$

where r_b is an average beam radius equal to the cathode radius; r_0 is the drift tube radius – anode radius (145 mm); V_0 is the multiplied voltage across the anode-cathode gap measured by the capacitive divider and equal to 0.25 MV. The formula presented above works for an annular beam, which is confirmed experimentally as shown on Fig. 2.

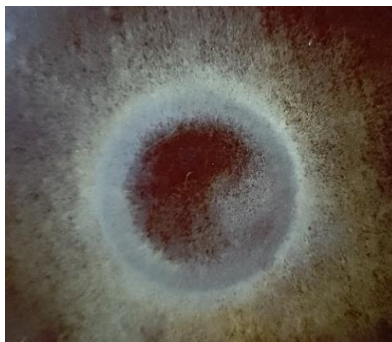


Fig. 2. Ring-shaped beam autograph

Hence, the limiting vacuum current ensures the VC formation.

The beam current value and the microwave radiation power are conditioned by the current values at the break time, the current decrease values during the break, and the rate of this process.

2. TECHNIQUE AND EXPERIMENTAL METHODS

By the break time, the current was I_{max} , the current decrease value at break (I_{break}) and the residual current ($I_{residual}$) were measured by Rogovski belt (RB) № 1 and the backup belt № 2, respectively. Both belts are coupled with the RC integrators of microsecond signals. The conversion factor of both belts is $1V = 1.2$ kA. Rogovski belt № 3 recorded the current flowing through the plasma jumper. It was placed at a distance of 140 mm behind the plasma guns from the side of the anode grid. In the case of a current break, by the moment when the jumper was already at the location of this belt, it recorded the total current of the beam and plasma. This belt operates in combination with a nanosecond RC integrator.

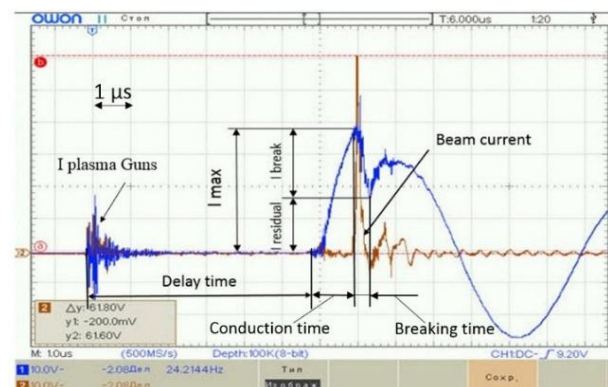


Fig. 3. Time diagram of current processes

The conversion coefficient is $1V = 0.282$ kA. Rogovski belt № 4 was used to record the beam current behind the anode grid at distances of 40 to 200 mm. This belt has the nanosecond RC integrator. The conversion coefficient is $1V = 0.275$ kA. The current of plasma guns was recorded by RB 15. The data from the belts were recorded by a four-channel WON XDS3104E oscilloscope with a bandwidth of 100 MHz and a sampling rate of 1 GSa/s.

A typical time diagram, the dynamics of currents measured by the above current meters, as shown in Fig. 3, makes it possible to identify specific sections that define the delay time between the operation of the PGs and the PCG (3 to 30 μs or more). The detailed description of the operation of plasma guns is given in article [11]. A minimum possible value of 3 μs is conditioned by the signal propagation time along the transmission lines and the response times of the discharger F2, the delay unit and the PCG start-up unit. The conduction time characterized by the front rise rate does not exceed 1.2 μs and is recorded by RB № 1. The current break time is within 200 ns and it is recorded by the RB № 1 or № 2. The duration of the beam current coincides with the break time and it is recorded by the RB № 3 or

RB № 4 built into the camera body. A quarter period of the current duration $T/4$ of plasma guns does not exceed $2 \mu\text{s}$ and it provides the implementation of a series of physical processes in the accelerator.

The charging voltage of PGs was varying in the range of 6 to 16 kV. The values below 6 kV failed to provide sufficient plasma density. And the values above 16 kV created the plasma concentration at which the current flowing through it was not able to break it. As a result, the current flowed through the jumper without the break of it and had a periodic character. The charging voltage at the PCG was varying in the range of 20 to 40 kV. Lower voltage values failed to provide the continuity of the break realization due to the impossibility of breaking the plasma jumper. Higher values were limited due to the observance of the electrical strength requirements set to the insulating structures of the accelerator.

For experiments with a time delay, the PCG and PG voltages had fixed values. When obtaining the dependences of the current on the charging voltage, for example, PCG, the time delay was fixed at the level of $6 \mu\text{s}$ and the PG voltage was recorded, etc. The generating pulses were launched at the same vacuum value of $p=5 \cdot 10^{-4}$ Torr. Each pulse with the same studied parameters was repeated 5 to 10 times.

3. EXPERIMENTAL PART

For the first time, the DIN-2K accelerator enabled the experimental generation of the current values at each stage of the facility operation starting with the PGs triggering through to the beam current formation behind the anode grid. Fig. 4 gives the oscillograms with the current break at a maximum that is an optimal mode and with the current break at an early front stage that is conventionally not optimal mode.

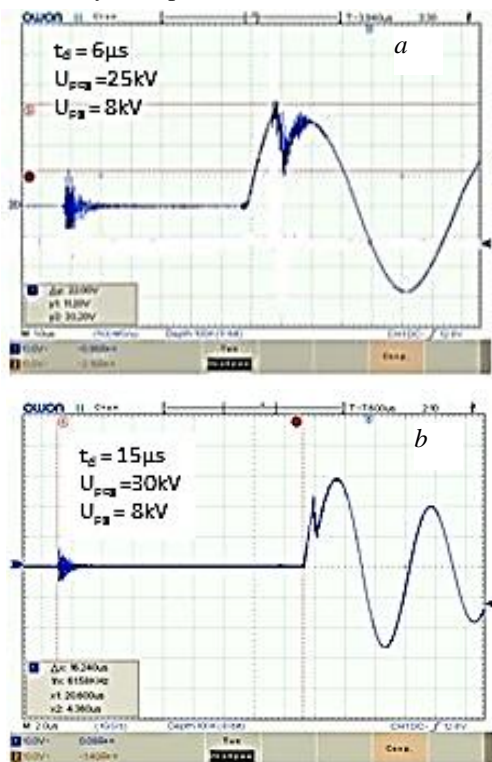


Fig. 4. The current break at a maximum (a), and at an early front stage (b)

Maximum values of the currents that are of interest for us were obtained for the cases similar to those of the shape of the current curve given in Fig. 4.a.

Fig. 5 gives the experimental dependence of the currents on the time delay in operation of the PGs and PCG.

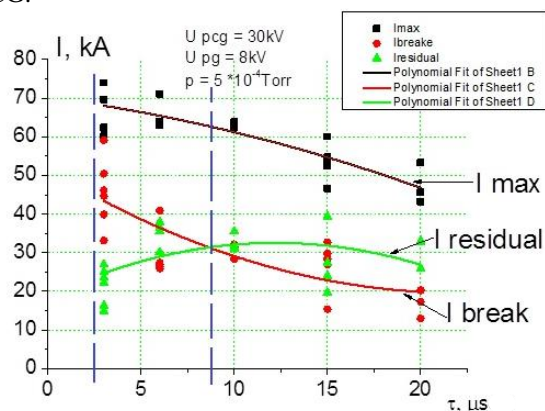


Fig. 5. Dependence of the current characteristics on the PGs and PCG time delays

The optimal section can be seen in the considered range of time delays when the current decrease value during the break (I_{break}) exceeds the residual current (I_{residual}) in plasma current breakers after the break. This domain is marked by a dotted line in the range of 3 to $7 \mu\text{s}$. Here, the current maxima are observed by the break time of 60 to 74 kA.

An increase in the maximum current does not necessarily provide an increase in the break current and, accordingly, does not lead to an expansion of the range of optimal values, or to its shift towards larger values (Fig. 6).

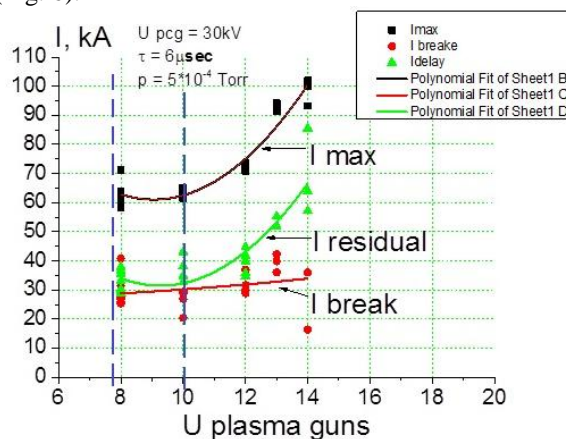


Fig. 6. The dependence of the current characteristics on the charging voltage of plasma guns at a fixed PCG voltage

In terms of the minimum residual current, the optimal voltage for a given PCG voltage is in the range of 8 to 10 kV. It can also be seen that with an increase in the current value by the time of the break, the energy input into the beam formation is decreased because most of the charge carriers remain uninvolved in the physical processes associated with the break. Hence, there is a need for an increase in the PCG charging voltage.

Fig. 7 shows that the optimal PCG charging voltage in terms of the minimum residual current is typical for the values exceeding 30 kV.

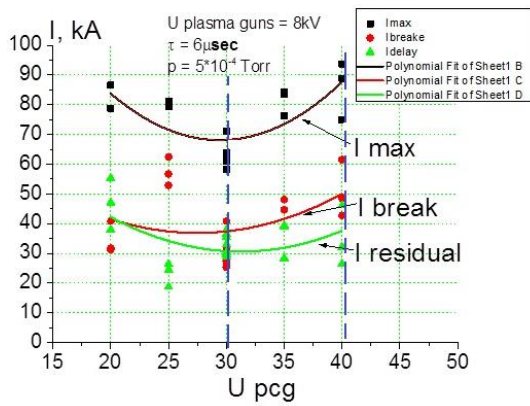


Fig. 7. The dependence of current characteristics on the PCG charging voltage at a fixed PG voltage

The difference between the break current and the residual current remains such that the break current is more than 50% of the maximum current value. Also, the plasma jumper breaks at the maximum, or close to the maximum (the moment of break occurs at a point above 85% of the peak current). The obtained dependences also show that optimal conditions arise at PCG voltages exceeding 30 kV. Here, the energy input to the current decrease value at the break is increased along with the current by the time of break.

When the break current was recorded, the values of the pulse strength in the beam formation region of about 4.8 GW were obtained for a maximum of the break current front, taking into account the fact that the measured anode-cathode voltage was 240 kV at the PCG charging voltage of 35 kV.

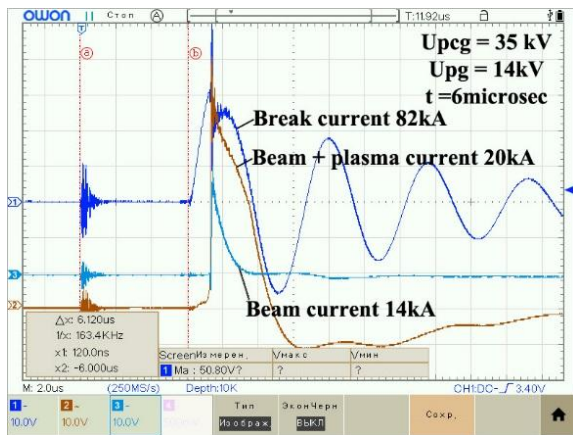


Fig. 8. Current characteristics, at $U_{pcg} = 35$ kV, $U_{pg} = 14$ kV and the delay time of 6 μ s

It can be seen (Fig. 8) that the beam current in the PCB domain and the beam current behind the VC domain at a distance of 40 mm from the grid significantly exceed the limiting vacuum current, and it should provide the availability of the current beam and the virtual cathode at given energy parameters of the primary circuit.

CONCLUSIONS

A system for diagnosing currents was created providing a sufficient level of accuracy and repeatability to define optimal operating modes for the DIN-2K accelerator. Optimal parameters for the operation of the DIN-2K accelerator were determined in terms of obtaining maximum current values by the time of break and

current decrease values at break. For the considered ranges of delay times and charging voltages of the PGs and PCG, it is reasonable to provide optimal current modes by changing PCG and PGs voltages, working at delays between the operation of the PGs and PCG of less than 8 μ s.

Each PCG charging voltage value corresponds to the optimal PG voltage value that provides the required plasma concentration and is selected experimentally. With an increase in the PCG voltage the PG voltage should also be increased in order to increase the values of the break current. Accordingly, each plasma density generated by the PG has a current initiated by the PCG that provides the best current break, the one that lies near the maximum.

REFERENCES

- O.V. Manuilenko, I.N. Onishchenko, A.V. Pashchenko, I.A. Pashchenko, V.B. Yuferov. Current Flow Dynamics in Plasma Opening Switch // *Problems of Atomic Science and Technology*. 2021, № 4, p. 6-10. <https://doi.org/10.46813/2021-134-006>.
- S.V. Loginov. Conduction Current in Low-Density Plasma Opening Switches // *IEEE Transactions on Plasma Science*. 2022, № 50(7), p. 2026-2029. <https://doi.org/10.1109/TPS.2022.3178792>.
- O.S. Druj, V.V. Yegorenkov, I.M. Onyshchenko, V.B. Yuferov. Plasma Dynamics in Accelerator with Plasma Opening Switch // *Problems of Atomic Science and Technology*. 2019, №6, p. 77-80. <https://doi.org/10.46813/2019-124-077>.
- O.S. Druj, V.V. Yegorenkov, A.V. Shchagin, V.B. Yuferov. Electron beam transport in dielectric tubes // *East European Journal of Physics*. 2014, v. 1, № 1, p. 70-73.
- V.B. Yuferov, E.I. Skibenko, I.V. Buravilov, A.S. Svichkar, A.N. Ponomarev, V.V. Katrechko, V.V. Nikulshina. SMALL-SIZE "DI-2" Accelerator with the Plasma Current Switch and Inductive Energy Accumulator as a Material Irradiation Test Rig // *Problems of Atomic Science and Technology*. 2022, № 4, p. 154-156. <https://doi.org/10.46813/2022-140-154>.
- U. Shanmuganathan, K. Saket, S. Senthil Kumar, M.K. Das, S. Nekkanti, S.K. Gupta, K. Senthil, V. Nallasamy. A Compact Repetitive Marx Generator for Generating Intense Electron Beams for HPM Sources // *IEEE Transactions on Electron Devices*. 2023, v. 70, № 3, p. 1256-1261. <https://doi.org/10.1109/TED.2022.3233810>.
- D.V. Vinnikov, I.V. Buravilov, V.B. Yuferov, A.N. Ponomarev, V.I. Tkachev. Linear Charged-Particle Accelerators Opportunities for the Use of the Small-Size Accelerator, VGIK-1 // *Problems of Atomic Science and Technology*. 2019, № 6, p. 115-121. <https://doi.org/10.46813/2019-124-115>.
- James Benford, John A. Swegle, Edl Schamiloglu. *High Power Microwaves*. CRC Press, 2015, 447 p.
- O.V. Manuilenko, I.N. Onishchenko, A.V. Pashchenko, I.A. Pashchenko, V.A. Soshenko, V.G. Svichensky, V.B. Yuferov, B.V. Zajtsev. Magnetic Field Dynamics in Plasma Opening Switch // *Problems of Atomic Science and Technology*. 2021, №6, p. 61-66. <https://doi.org/10.46813/2021-136-061>.

10. O.V. Manuilenko, I.N. Onishchenko, A.V. Pashchenko, I.A. Pashchenko, V.B. Yuferov. Plasma and Magnetic Field Dynamics in POS: PIC simulations // *Problems of Atomic Science and Technology*. 2022, № 6, p. 55-59. <https://doi.org/10.46813/2022-142-055>.

11. D.V. Vinnikov, V.V. Katrechko, V.B. Yuferov, V.I. Tkachev. Plasma Guns of an Erosion Type with the Pulse-Periodic Gas-Metal Injection // *Problems of Atomic Science and Technology*. 2022, № 6, p. 60-65. <https://doi.org/10.46813/2022-142-060>.

Article received 23.06.2023

ВПЛИВ ЕНЕРГЕТИЧНИХ ПАРАМЕТРІВ ПЕРВИННОГО КОНТУРУ НА СТРУМОВІ ХАРАКТЕРИСТИКИ ПРИСКОРЮВАЧА ДІН-2К

Д.В. Вінніков, В.В. Катречко, О.М. Озеров, В.І. Ткачов, С.В. Марченко, В.Б. Юферов, О.В. Мануйленко

Встановлено оптимальні значення напруги для плазмових гармат і генератора імпульсного струму, що забезпечують максимальні значення струму розриву. Значення струму визначено для області формування плазмової перемички. Встановлено оптимальну затримку часу між спрацьовуванням плазмових гармат і генератора імпульсного струму. Струм пучка вимірювався в області за вакуумним діодом і в області плазмової перемички. Граничний струм був визначений для наявної геометрії установки.